Superexchange-mediated negative thermal expansion in Nd-doped $BiFeO_3$

Christopher M. Kavanagh, Philip Lightfoot and Finlay D. Morrison*

School of Chemistry and EaStCHEM, University of St Andrews, St Andrews, KY16 9ST, United Kingdom

Electronic Supplementary Information

Table S1: Goodness-of-fit parameters for magnetic and non-magnetic refinements of the *Pnma* model at 100 K.

Magnetic Symmetry	**Space group**	χ^2	wR_p	R_p
G_z	*Pn'ma'*	9.552	0.0971	0.0802
G_y	*Pn'm'a*	11.810	0.1080	0.0962
G_x	*Pnma*	11.860	0.1820	0.0947
(non-magnetic)	*Pnma*	13.090	0.1137	0.1047

Table S2: Goodness-of-fit parameters for refinements with and without L_{xx} strain terms.

Model	**Spacegroup**	χ^2	wR_p	R_p
No strain terms	*Pn'ma'*	8.647	0.0925	0.0763
Profile 3 L_{33}	*Pn'ma'*	5.19	0.0717	0.0626
Profile 3 L_{33} L11	*Pn'ma'*	4.898	0.0696	0.0624
Profile 3 L_{xx} (6 terms)	*Pn'ma'*	3.522	0.059	0.0536

Table S3: The freezing temperatures and associated errors for are shown for fixed values of f_0 as obtained from Vogel-Fulcher fits of permittivity data.

f_0 **(Hz)**	**ln** f_0	T_f**(K)**	E_a**(eV)**	χ^2	R^2
10^9	20.7	126.1 ± 0.7	0.02 ± 0.01	5.88×10^{-2}	0.985
10^{12}	27.6	110.7 ± 0.7	0.057 ± 0.001	1.76×10^{-2}	0.996

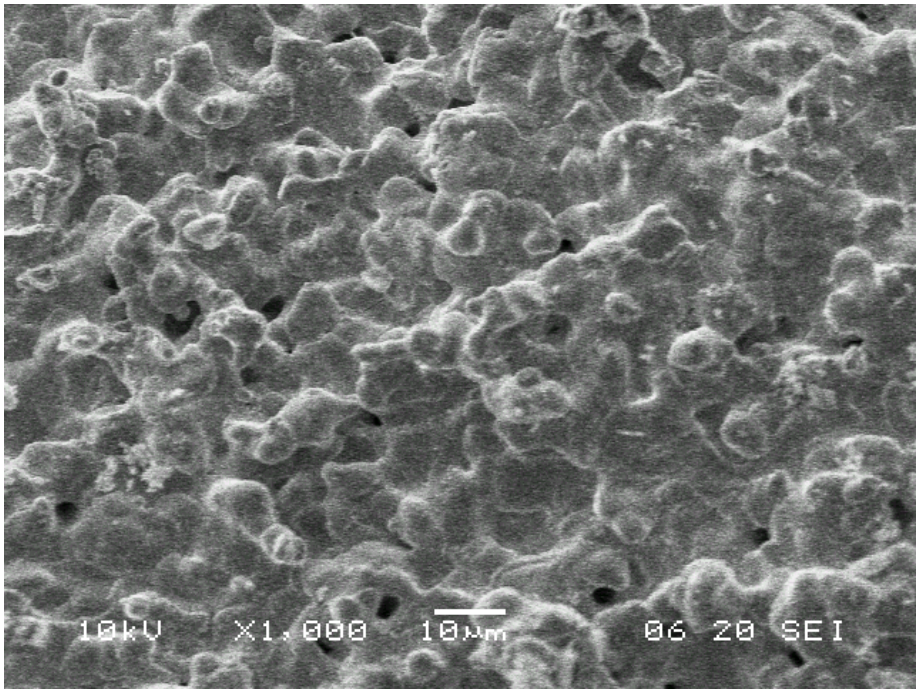

Figure S1: Scanning electron micrograph of $Bi_{0.7}Nd_{0.3}FeO_3$ pellets sintered at 1000 °C.

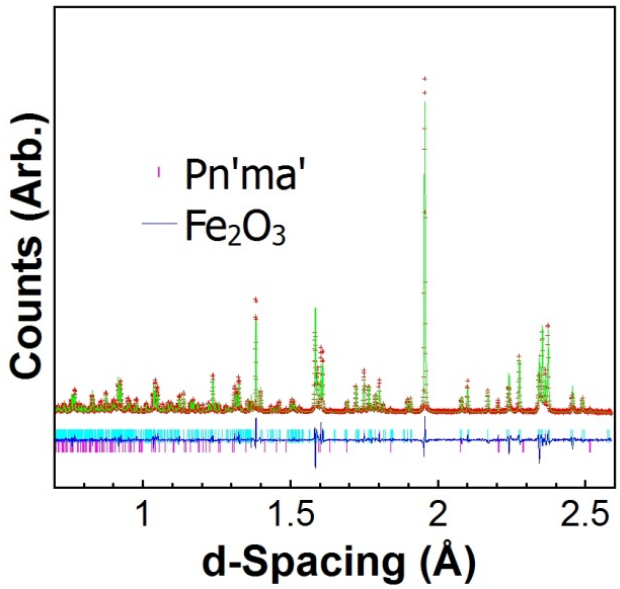

Figure S2: Isotropic refinement of the 50 K PND data showing a poor quality of fit due to the modelling of peak shapes; $\chi^2 = 8.647$, $wRp = 0.0925$, $Rp = 0.0763$.

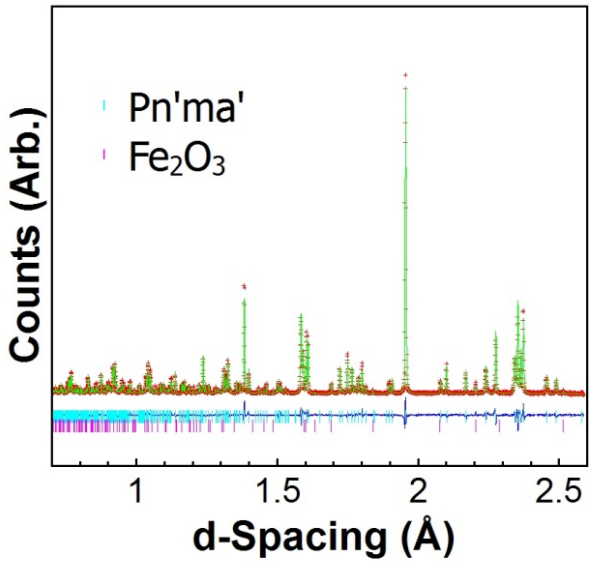

Figure S3: Refinement profile of the 50 K data with anisotropic L_{33} and L_{11} peak broadening terms; $\chi^2 = 4.898$, $wR_p = 0.0696$ $R_p = 0.0624$.

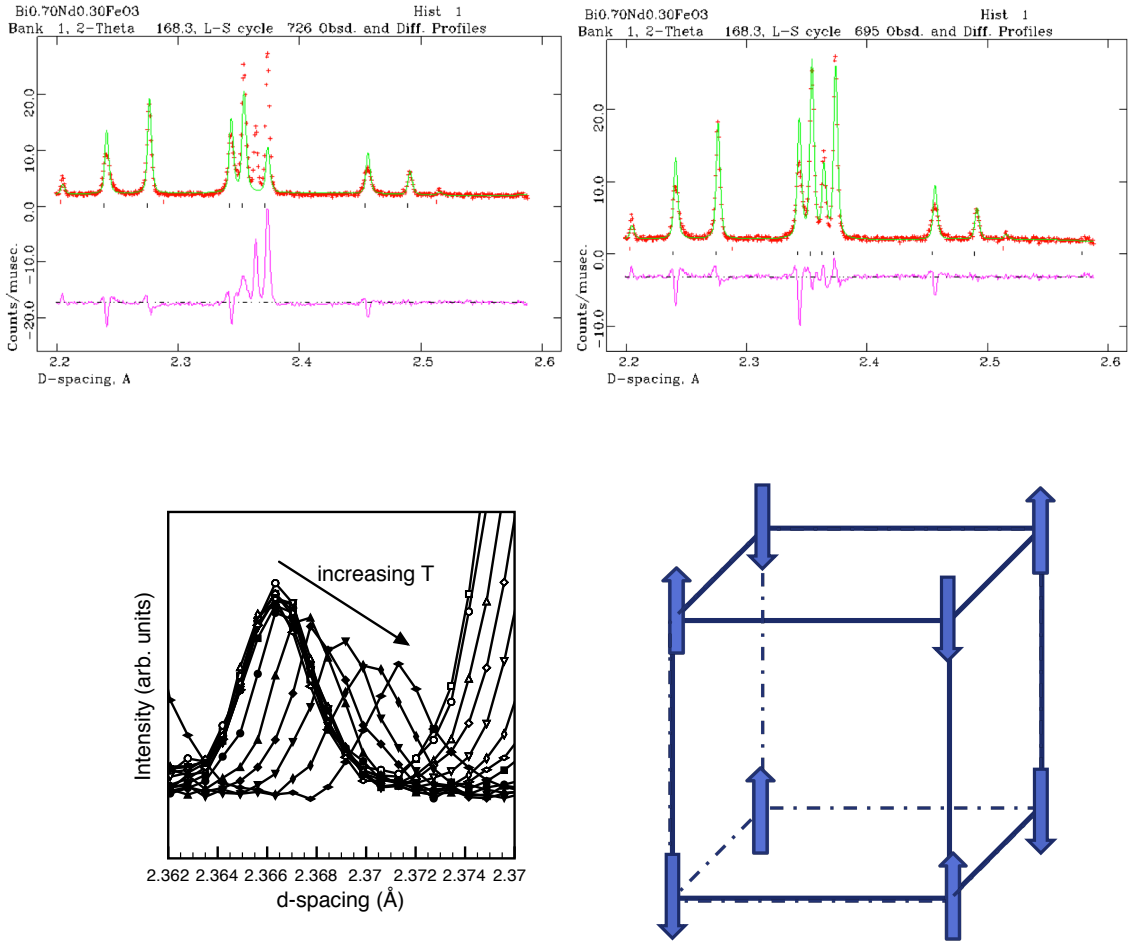

Figure S4: Rietveld refinement profiles of ND data at 50 K without (top left) and with (top right) the magnetic cell included. Note the purely magnetic (130) reflection at 2.36 Å. Temperature dependence of the (130) magnetic reflection (bottom left) over the range 50 to 500 K; representation of G_z type antiferromagnetic ordering (bottom right), where the moments are aligned along the z-axis and arranged in an antiparallel arrangement with respect to nearest neighbours in all three (*x*,*y*,*z*) axes.

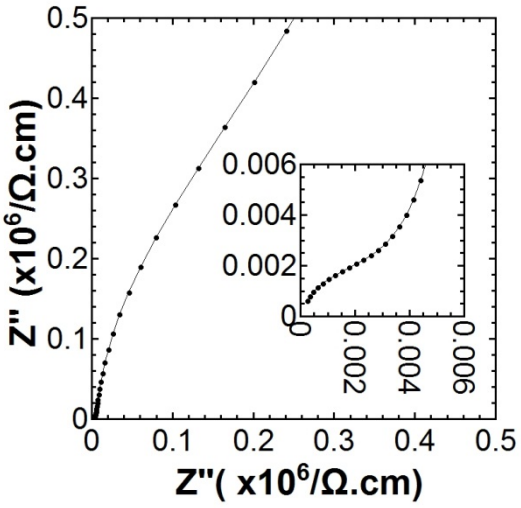

Figure S5: Complex impedance, Z^*, plane plot at 280 K showing the grain boundary and conducting bulk response (inset).

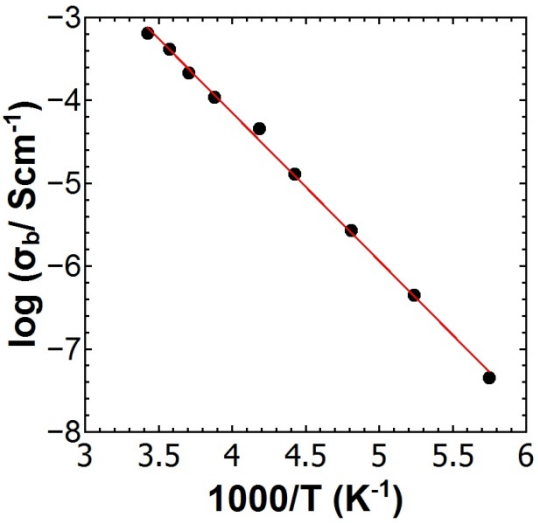

Figure S6: Arrhenius plot of bulk conductivities determined from M^* data; $E_a = 0.35 \pm 0.01$ eV ($R^2 = 0.998$).

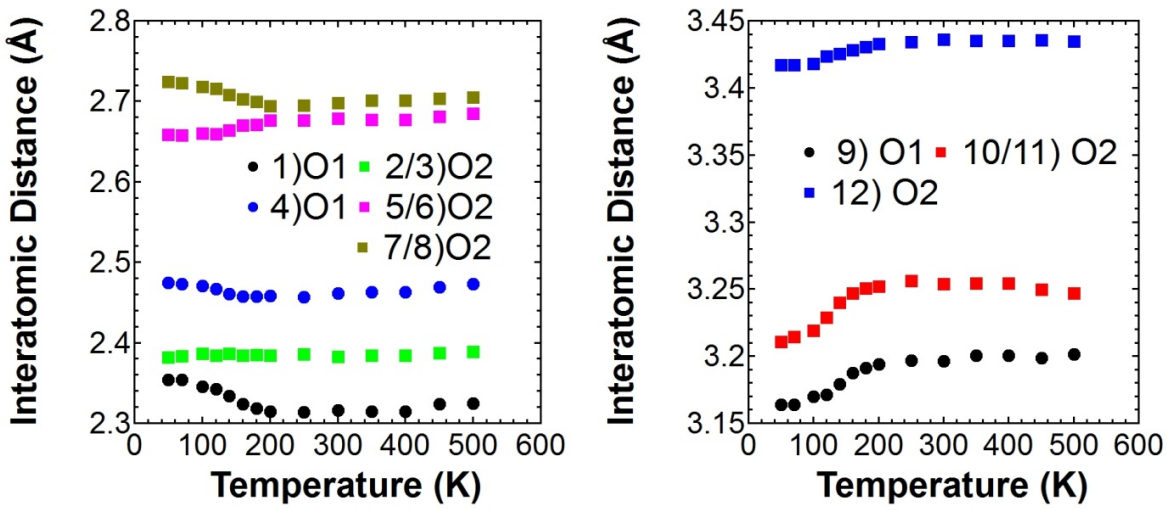

Figure S7: Interatomic distances between the A-site and axial (O1) and equatorial oxygens (O2)

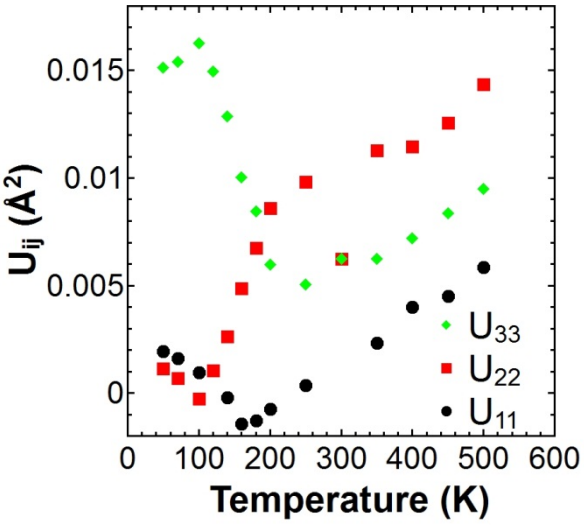

Figure S8: A-site anisotropic atomic displacement parameters (U_{ij}) as a function of temperature along *a* (U_{11}), *b* (U_{22}), and *c* (U_{33}) axes.